

Modeling the Effect of Node Synchronization Times in Ultra Wideband Wireless Networks

Christopher S. Taggart, Yannis Viniotis and Mihail L. Sichitiu

*Department of Electrical and Computer Engineering,
North Carolina State University,
Raleigh, NC 27695-7911*

Abstract

Ultra-wideband wireless (UWB) can provide the physical layer for high-throughput personal area networks. When UWB is used for communication between many nodes, relatively long acquisition times are needed when dropping and re-establishing wireless links between the nodes. This paper describes the development and use of mathematical and simulation models to investigate the impact of dropping and reacquiring links between nodes on average packet delay; we also consider the performance of the alternative strategy of forwarding packets through intermediate nodes without breaking the established wireless links. The work presented here assumes that no specific MAC layer protocol, such as WiMedia UWB MAC, is operating. The paper describes the models, explains the selection of modeling parameters used, compares the average packet delay for a network of three simple UWB nodes and for a ring of ten UWB nodes and explains the use of these results for network design engineers.

Key words: Ultra-wideband, average delay, simulation, servers with vacations
PACS:

1 Introduction

This paper expands upon research originally published in (Taggart et al., 2007) that describes conceptual, mathematical, and simulation models for a simple data network. The expansion includes consideration of a ring network of ten

Email addresses: cstaggar@ncsu.edu (Christopher S. Taggart,),
candice@ncsu.edu (Yannis Viniotis and), mlsichit@ncsu.edu (Mihail L. Sichitiu).

nodes in which one of the nodes may switch links between its normal downstream neighbor and the node opposite on the ring. The nodes in the model use ultra-wideband (UWB) wireless as the physical layer, requiring relatively long node acquisition times when links are dropped and reestablished. For the first case, only three nodes are considered and each has only one input and one output link. We use the models to study average packet delay for two models of network operation. In the first model, the three nodes are connected in tandem and packets destined for the last node are forwarded through the second node. In the second model, the first node drops synchronization with the second node and establishes a link with the third node to send any packet bound for the third node. For the second case, the models are extended to a ten node ring network. This network is set up to allow one node to occasionally stop sending to its downstream neighbor and begin sending packets to the node on the opposite side of the ring. We present a mathematical model of average delay as a function of network parameters and node acquisition time for this case and compare this model to preliminary simulation model results.

The short pulse lengths used in UWB communications require relatively long synchronization times between the receiver and transmitter - from microseconds (ISO, 2007) to milliseconds (Roy et al., 2004). Finding ways to shorten this synchronization time is an ongoing research area (Aedudodla et al., 2004) and (Aedudodla et al., 2006).

Because of the relatively long acquisition times, it is not practical for a high data rate source to frequently switch between two destinations. Figure 1 depicts two different strategies for networking a source S and two destinations D_1 and D_2 . In Fig. 1(a), the traditional approach is depicted with the source sending packets to both destinations, alternating transmissions between them. In Fig. 1(b), the source directs all traffic to the first destination which, in turn, forwards the traffic to the second destination. The strategy in Fig. 1(a) is commonly employed in wireless networks. However, in UWB, the source must acquire each new destination node, synchronizing with the receiver before it can start data transmission, a potentially very expensive (in terms of efficiency) proposition. Therefore, it is very likely that in UWB the scheme depicted in Fig. 1(b) will be far more efficient than the scheme in Fig. 1(a).

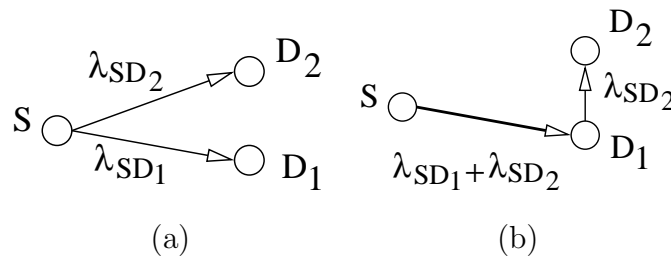


Fig. 1. Two options to transfer information from source S to two different destinations D_1 and D_2

If M transceivers are used for each node, M distinct links can be maintained and used without the overhead of resynchronization. However, such a node is significantly more complex and potentially expensive. In this paper, we focus on nodes with a single transceiver. Hence, each network node can send to a single destination and receive from a single source. In previous work (Taggart et al., 2005), we showed that minimum delay is achieved by forming nodes into rings and apportioning the aggregate capacity available to each link in proportion to offered load.

2 Models

2.1 The Conceptual Models

The conceptual models of the operation of the three node network with packet forwarding and with link switching can be best explained through diagrams with explanatory remarks. The concept of operation for the ten node network, essentially an extension of the three node network model, is explained in the same fashion.

2.1.1 Three Node Packet Forwarding Operation

Understanding the operation of the packet forwarding model is important because packet forwarding is common and useful in ad hoc networks, providing a convenient alternative to requiring nodes to drop and reacquire each other to send data packets. Figure 2 shows the conceptual model for a three node network operating solely in a packet forwarding mode. Node 1 sends all traffic to Node 2. Node 2 keeps its own traffic while forwarding traffic bound for Node 3, which includes packets from Nodes 1 and 2. In this network set up, the existing wireless links are used - dropping of links and reacquisition is not performed because link switching is not required.

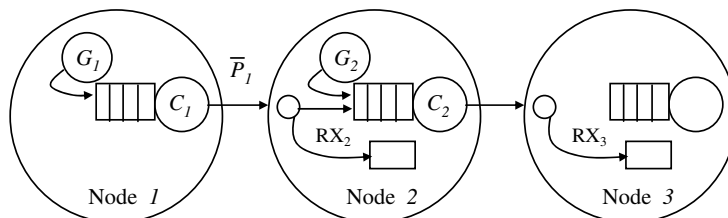


Fig. 2. Three node packet forwarding diagram

We define a network of three wireless nodes, each of which is always within wireless range of the others. Each node generates its own traffic and routes

traffic received from other nodes. Each node i has one incoming wireless link and one outgoing wireless link. Nodes 1 and 2 generate packets exponentially distributed in time with an average packet generation rate of G_i packets per second, which is defined as

$$G_1 = \lambda_{12} + \lambda_{13}, \quad (1)$$

$$G_2 = \lambda_{23}. \quad (2)$$

Nodes 1 and 2 have packet queues of infinite size and serve packets such that the inter-service intervals are exponentially distributed with an average service rate of c_i packets per second. Arriving packets with destination i are received at an average rate of RX_i . The average traffic on the incoming link to node i is given by \bar{P}_i . Arriving packets destined for other nodes are immediately queued for forwarding. Node 3 neither generates nor queues packets, but simply receives packets at an average rate of RX_3 .

2.1.2 Three Node Switching Operation

As discussed, the alternative to simply forwarding packets from node 1 to node 3 via node 2 is to allow node 1 to drop its link with node 2, acquire and establish a new link with node 3, and forward packets from Node 1 directly to Node 3. The network set-up is provided in Fig. 3 below.

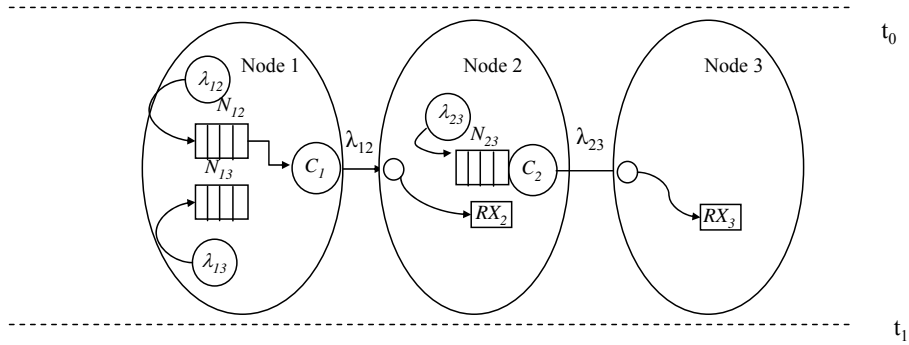


Fig. 3. Three node network switching diagram

Node 1 contains two queues served by a single server with exponentially distributed service times. The average rate of packet service is c_1 , with the server being shared between the two queues. Each queue is fed by packet generators with exponentially distributed generation times with averages λ_{12} and λ_{13} , where λ_{ij} is the average rate, in packets per second, of traffic originating at node i and destined for node j .

Node 2 contains only a single queue and server, with packet generation and

service times exponentially distributed at average rates λ_{23} and c_2 , respectively. Node 3 simply receives packets for which it is the destination. In this model, all packets from Node 2 have Node 3 as their destination. Packets from Node 1 may have Node 2 or Node 3 as their destination.

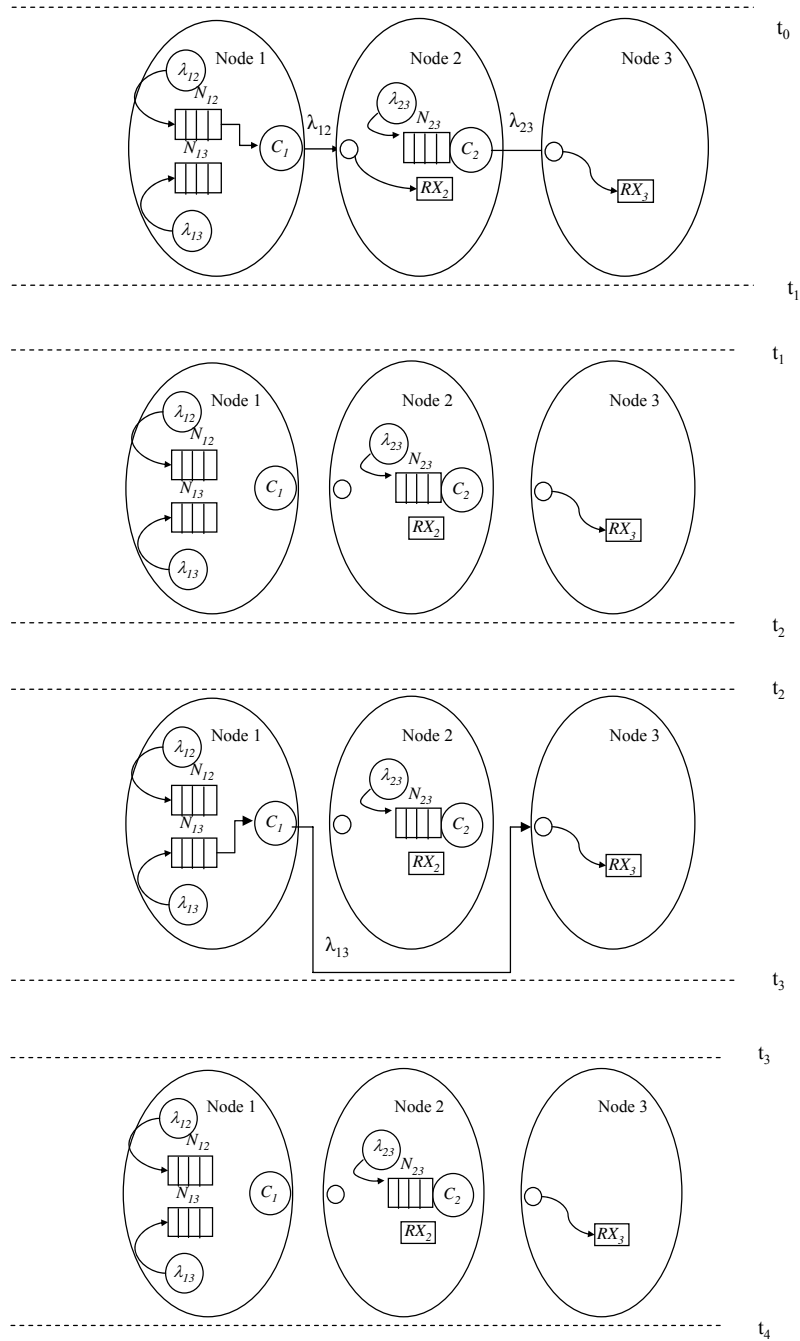


Fig. 4. Queue operation as nodes switch and reacquire wireless links

Figure 4 shows how the queue behavior changes during system operation. From t_0 to t_1 , the server in Node 1 serves only the queue with packets destined for

Node 2. We will call this queue Q_{12} . The queue with packets destined for Node 3 (Q_{13}) simply fills up during this time because the Node 1 server is busy serving Q_{12} .

Meanwhile, Q_{23} in Node 2 is served by the Node 2 server and packets are forwarded to Node 3. At Node 3, packets are simply received with no additional delay. The nodes continue in this state until the size of Q_{12} drops below a lower threshold, NT_{low} .

From t_1 to t_2 , the nodes are synchronizing as part of the link acquisition process and no packets are served in any queue. (Later, we will define and use the synchronization time, t_{synch} , related to this synchronization event.) Again, all queues just fill up because packets are being generated but not served in each queue.

From t_2 to t_3 , Node 1 has acquired Node 3 and is sending packets from Q_{13} . Q_{12} and Q_{23} are not being served, so they just fill up. Service continues in this manner until the queue size of Q_{13} drops below a lower threshold, NT_{low} .

Finally, from t_3 to t_4 , the nodes synchronize wireless links again during acquisition and all queues fill during the synchronization period. The stages of this process repeat for future time increments. During the time represented in Fig. 4, synchronization between network nodes occurs twice.

2.1.3 Ten Node Packet Forwarding Operation

In previous work (Taggart et al., 2005), we developed a mathematical model for determining average packet delay in a ring network of UWB nodes. In this model, each node generates packets exponentially distributed in time with an average packet generation rate of G_i packets per second. Each node has a single packet queue of infinite size and serves packets with exponentially distributed inter-service intervals with an average service rate of c_i packets per second. Arriving packets with destination i are received at an average rate of RX_i . Arriving packets destined for other nodes are immediately queued for forwarding. A block diagram of a node from this network is depicted in Fig. 5.

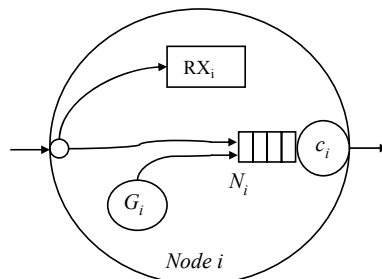


Fig. 5. Block diagram of a network node

2.1.4 Ten Node Switching Operation

For the ten node network, Node 3 occasionally switches between sending packets on to Node 7 and sending packets to Node 8. This behavior requires Node 3 to have a different physical structure than other nodes. As shown in Fig 6, Node 3 must have a queue for each half of the network. One queue holds packets destined for Nodes 1, 2, 8, 9, and 10 and is termed the top half queue. The other queue holds packets destined for Nodes 4, 5, 6, and 7 and is called the bottom half queue. The top half queue has a low threshold N_3^L and a high threshold, N_3^H . These values are used to control Node 3 switching in the network.

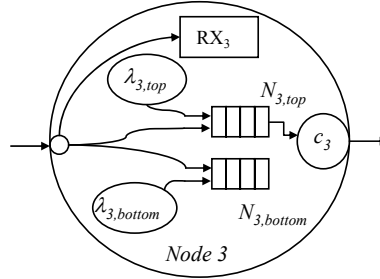


Fig. 6. Block diagram of Node 3

The sequence of operations is shown in Fig. 7. Here is how this network operates:

- (t_0 to t_1) All nodes forward packets normally. Node 3 holds packets for top half (Nodes, 1, 2, 8, 9, 10) until the top half queue reaches the high threshold value, N_3^H .
- (t_1 to t_2) Node 3 signals Node 7 to stop sending to Node 8. Node 7 acknowledges the order from Node 3. Node 3 stops sending packets to Node 4. Node 7 stops sending packets to Node 8.
- (t_2 to t_3) Node 3 stops sending to Node 4. Node 3 acquires Node 8.
- (t_3 to t_4) Node 3 sends packets to Node 8 until the top half queue reaches the low threshold, N_3^L .
- (t_4 to t_5) Node 3 stops sending to Node 8. Node 3 acquires Node 4.
- (t_5 to t_6) Node 3 signals Node 7 to acquire Node 8. Node 7 acquires Node 8.
- (t_6 to t_7) Node 7 signals Node 3 that it has acquired Node 8. Node 3 waits for Node 7 acknowledgement before sending data. Behavior continues with the same events as in t_0 to t_1 .

From Figure 7, we define four states: Node 3 sending to Node 4, Acquisition, Node 3 sending to Node 8, and Waiting. The durations of each state are also shown in Figure 7 and will be used later in delay calculations for the ten node switching model.

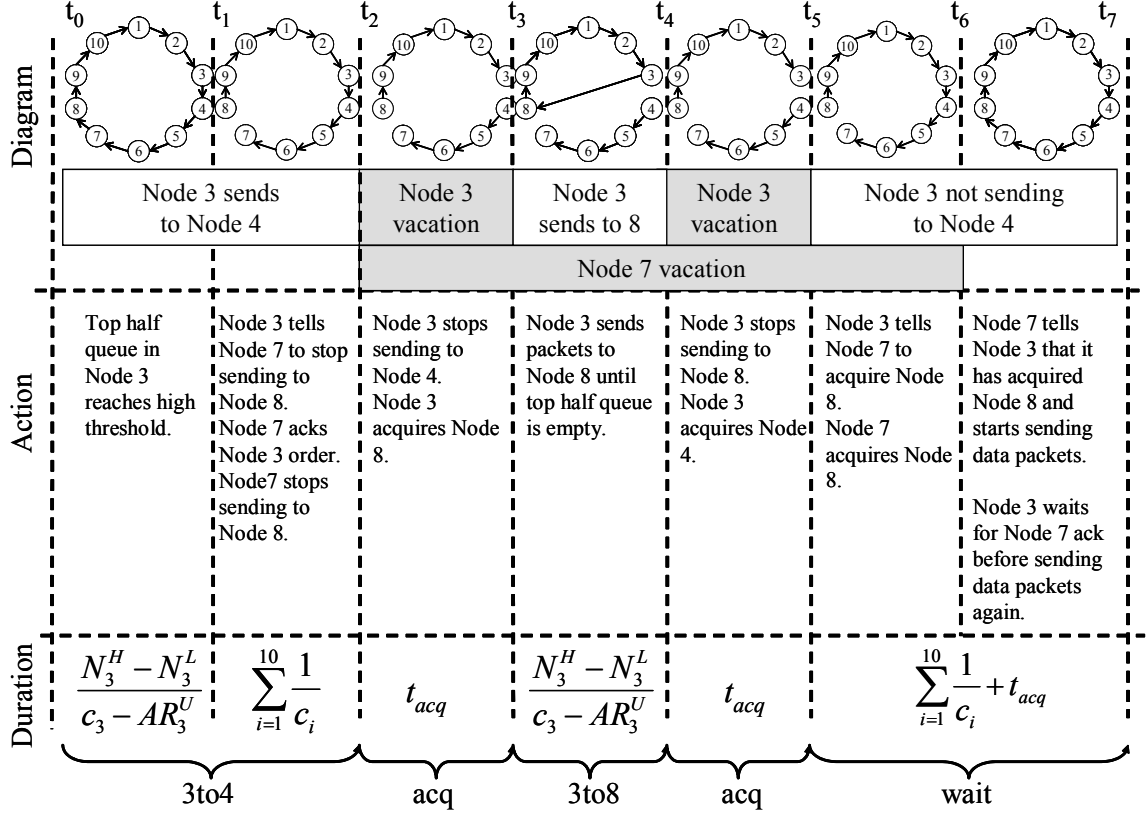


Fig. 7. The states of network operation used for calculating average delay

2.2 The Mathematical Models

We draw heavily from queuing theory to develop mathematical models for the average packet delay for the packet forwarding and the switching network models.

2.2.1 Three Node Packet Forwarding Operation

Approximating the queues as $M/M/1$ systems, we can write for the average system delays:

$$\bar{T}_1 = \frac{1}{c_1 - \lambda_{12} - \lambda_{13}} \quad (3)$$

$$\bar{T}_2 = \frac{1}{c_2 - \lambda_{13} - \lambda_{23}}. \quad (4)$$

Keeping in mind that packets generated in Node 1 that are bound for Node 3 must wait in both the Node 1 and Node 2 queues, we obtain the expression

for average packet delay:

$$\begin{aligned}
\bar{T}_{forwarding} = & \frac{\lambda_{12}}{\sum_{12,13,23} \lambda_{ij}} \left(\frac{1}{c_1 - \lambda_{12} - \lambda_{13}} \right) + \\
& + \frac{\lambda_{13}}{\sum_{12,13,23} \lambda_{ij}} \left(\frac{1}{c_1 - \lambda_{12} - \lambda_{13}} + \right. \\
& \left. + \frac{1}{c_2 - \lambda_{13} - \lambda_{23}} \right) + \\
& + \frac{\lambda_{23}}{\sum_{12,13,23} \lambda_{ij}} \left(\frac{1}{c_2 - \lambda_{13} - \lambda_{23}} \right)
\end{aligned} \tag{5}$$

For comparison with the behavior of the switching model, we develop delay equations for the special case of a homogeneous network where the packet generation and service rates for all nodes are the same. That is, $G_i = G$ and $c_i = c$.

Substituting λ for λ_{ij} and c for c_i as described above, we obtain:

$$\bar{T}_{forwarding} = \frac{\lambda}{3\lambda} \left(\frac{1}{c - 2\lambda} \right) + \frac{\lambda}{3\lambda} \left(\frac{2}{c - 2\lambda} \right) + \frac{\lambda}{3\lambda} \left(\frac{1}{c - 2\lambda} \right), \tag{6}$$

which reduces to:

$$\bar{T}_{forwarding} = \frac{4}{3} \frac{1}{c(1 - 2\rho)}, \tag{7}$$

where $\rho = \lambda/c$. Later in the paper, we will use this homogeneous network model to compare delays between the packet forwarding model and the link switching model.

2.2.2 Three Node Switching Operation

For the node switching model, the time interval for each period can be approximated by the equations shown in Table 1. Here, $N_{ij}(t_k)$ represents the number of packets in queue ij at time t_k . Synchronization time, t_{synch} , is the time it takes for a node to drop wireless synchronization with one node and establish a new wireless link with the other node and is assumed to be a constant for this analysis. We also make the steady state assumption that queue sizes for each queue are the same at the beginning and end of this switching and synchronization cycle.

Using Little's law and Table 1, we define a series of iterative equations to approximate the number of packets in each queue at each time, t_0 to t_4 . Then,

Table 1
Queue service status and time intervals

Period	In Service	Duration Approximation
$t_0 - t_1$	Q_{12}, Q_{23}	$t_1 - t_0 = \frac{N_{12}(t_0) - NT_{low}}{c_1 - \lambda_{12}}$
$t_1 - t_2$	None	$t_2 - t_1 = t_{synch}$
$t_2 - t_3$	Q_{13}	$t_3 - t_2 = \frac{N_{13}(t_2) - NT_{low}}{c_1 - \lambda_{13}}$
$t_3 - t_4$	None	$t_3 - t_4 = t_{synch}$

in order to obtain a solution for the steady state situation, we set $N_{12}(t_4)$ equal to $N_{12}(t_0)$ and $N_{13}(t_4)$ equal to $N_{13}(t_0)$. This condition states that at the time we observe the system of queues, the number of packets in Q_{12} and Q_{13} is stable over a complete cycle of switching service and the required synchronization between nodes for wireless link establishment.

At time t_1 , N_{12} has reached the low threshold at which switching must begin so

$$N_{12}(t_1) = NT_{low}. \quad (8)$$

Synchronization occurs during t_1 to t_2 with no queues being served, so we can approximate

$$N_{12}(t_2) = NT_{low} + \lambda_{12}t_{synch}. \quad (9)$$

Applying the iterative equations and the steady state condition to the queue sizes for Q_{12} and Q_{13} , yields the approximations in Table 2.

Table 2
Switching model queue size approximations

Q_{12} size	Q_{13} size
$N_{12}(t_0) = N_{12}(t_3) + \lambda_{12}t_{synch}$	$N_{13}(t_0) = N_{13}(t_3) + \lambda_{13}t_{synch}$
$N_{12}(t_1) = NT_{low}$	$N_{13}(t_1) = N_{13}(t_0) + \lambda_{13}(t_1 - t_0)$
$N_{12}(t_2) = N_{12}(t_1) + \lambda_{12}t_{synch}$	$N_{13}(t_2) = N_{13}(t_1) + \lambda_{13}t_{synch}$
$N_{12}(t_3) = N_{12}(t_2) + \lambda_{12}(t_3 - t_2)$	$N_{13}(t_3) = NT_{low}$
$N_{12}(t_4) = N_{12}(t_3) + \lambda_{12}t_{synch}$	$N_{13}(t_4) = N_{13}(t_3) + \lambda_{13}t_{synch}$

These simultaneous linear equations can be solved in the standard way, noting that there are only two independent variables, $N_{12}(t_0)$ and $N_{13}(t_2)$.

Starting with the equations in Table 2, we write

$$\begin{aligned}
N_{12}(t_0) &= N_{12}(t_3) + \lambda_{12}t_{synch} \\
&= N_{12}(t_2) + \lambda_{12}(t_3 - t_2) + \lambda_{12}t_{synch} \\
&= NT_{low} + 2\lambda_{12}t_{synch} + \lambda_{12}\left(\frac{N_{13}(t_2) - NT_{low}}{c_1 - \lambda_{13}}\right)
\end{aligned} \tag{10}$$

Simplifying and regrouping, we obtain:

$$\begin{aligned}
N_{12}(t_0) &= \left(\frac{\lambda_{12}}{c_1 - \lambda_{13}}\right)N_{13}(t_2) + 2\lambda_{12}t_{synch} \\
&+ NT_{low}\left(1 - \frac{\lambda_{12}}{c_1 - \lambda_{13}}\right).
\end{aligned} \tag{11}$$

In a similar fashion, we obtain for $N_{13}(t_2)$:

$$\begin{aligned}
N_{13}(t_2) &= \left(\frac{\lambda_{13}}{c_1 - \lambda_{12}}\right)N_{12}(t_0) + 2\lambda_{13}t_{synch} \\
&+ NT_{low}\left(1 - \frac{\lambda_{13}}{c_1 - \lambda_{12}}\right).
\end{aligned} \tag{12}$$

Solving these equations simultaneously yields:

$$N_{12}(t_0) = NT_{low} + 2\lambda_{12}t_{synch}\left[\frac{(c_1 - \lambda_{12})}{c_1 - \lambda_{12} - \lambda_{13}}\right], \tag{13}$$

and

$$N_{13}(t_2) = NT_{low} + 2\lambda_{13}t_{synch}\left[\frac{c_1 - \lambda_{13}}{c_1 - \lambda_{12} - \lambda_{13}}\right]. \tag{14}$$

Using these equations, we solve for the time intervals $t_1 - t_0$ and $t_3 - t_2$ and because $t_2 - t_1$ and $t_4 - t_3$ are both synchronization periods, we obtain the results in Table 3.

Table 3

Switching model time duration approximations

Duration	Expression
$t_1 - t_0$	$\frac{2\lambda_{12}t_{synch}}{c_1 - \lambda_{13} - \lambda_{12}}$
$t_2 - t_1$	t_{synch}
$t_3 - t_2$	$\frac{2\lambda_{13}t_{synch}}{c_1 - \lambda_{13} - \lambda_{12}}$
$t_4 - t_3$	t_{synch}

We uses results from $M/M/1$ queues with service vacations to approximate the average system delays.

Let V_1, V_2, \dots be durations of successive vacations for an M/G/1 queue, where vacation durations are assumed to be independent and identically distributed.

From (Bertsekas and Gallager, 1992), (Scholl and Kleinrock, 1983), the expected system delay is:

$$\bar{T} = \bar{X} + \frac{\lambda \bar{X}^2}{2(1-\rho)} + \frac{\bar{V}^2}{2\bar{V}}, \quad (15)$$

where λ is the average arrival rate in the queue, \bar{X} is the average service time for the server, \bar{X}^2 is the second moment of the average service time, \bar{V} is the average vacation duration, and \bar{V}^2 is the second moment of the average vacation duration.

For our model, the duration of the server vacations is a constant. For queue Q_{12} , the duration of server vacations is the sum of the time needed for the nodes to synchronize, the time for queue Q_{13} to empty to the low threshold value NT_{low} , and the time for the nodes to synchronize again.

$$V_{12} = 2t_{synch} + \frac{N_{13}(t_2) - NT_{low}}{c_1 - \lambda_{13}}, \quad (16)$$

which reduces to

$$V_{12} = 2t_{synch} \left(\frac{c_1 - \lambda_{12}}{c_1 - \lambda_{12} - \lambda_{13}} \right). \quad (17)$$

Similarly,

$$V_{13} = 2t_{synch} \left(\frac{c_1 - \lambda_{13}}{c_1 - \lambda_{12} - \lambda_{13}} \right), \quad (18)$$

and, because queues Q_{12} and Q_{23} are "on vacation" for the same duration,

$$V_{23} = 2t_{synch} \left(\frac{c_1 - \lambda_{12}}{c_1 - \lambda_{12} - \lambda_{13}} \right). \quad (19)$$

For a constant, c ,

$$\bar{c} = c, \quad (20)$$

and

$$\overline{c^2} = c^2, \quad (21)$$

therefore we can express the waiting time in queue Q_{12} as follows:

$$\bar{T}_{12}(t_0 \rightarrow t_4) = \frac{1}{c_1} + \frac{\lambda_{12}}{c_1(c_1 - \lambda_{12})} + t_{synch} \left(\frac{c_1 - \lambda_{12}}{c_1 - \lambda_{12} - \lambda_{13}} \right). \quad (22)$$

The delays for queues with vacations Q_{13} and Q_{23} can be calculated in a similar fashion yielding:

$$\bar{T}_{13}(t_0 \rightarrow t_4) = \frac{1}{c_1} + \frac{\lambda_{13}}{c_1(c_1 - \lambda_{13})} + t_{synch} \left(\frac{c_1 - \lambda_{13}}{c_1 - \lambda_{12} - \lambda_{13}} \right), \quad (23)$$

and

$$\bar{T}_{23}(t_0 \rightarrow t_4) = \frac{1}{c_2} + \frac{\lambda_{23}}{c_2(c_2 - \lambda_{23})} + t_{synch} \left(\frac{c_1 - \lambda_{12}}{c_1 - \lambda_{12} - \lambda_{13}} \right). \quad (24)$$

Using the average delay for each queue, we compute the overall average delay for the network by taking the weighted average of the average queue delays with respect to the number of packets generated in each queue:

$$\begin{aligned} \bar{T}_{overall}(t_0 \rightarrow t_4) &= \frac{N_{12}^{total}}{N_{total}} \bar{T}_{12}(t_0 \rightarrow t_4) \\ &\quad + \frac{N_{13}^{total}}{N_{total}} \bar{T}_{13}(t_0 \rightarrow t_4) \\ &\quad + \frac{N_{23}^{total}}{N_{total}} \bar{T}_{23}(t_0 \rightarrow t_4), \end{aligned} \quad (25)$$

where

$$N_{ij}^{total} = \lambda_{ij}(t_4 - t_0), \quad (26)$$

and

$$N_{total} = N_{12}^{total} + N_{13}^{total} + N_{23}^{total}. \quad (27)$$

Using these equations, we can calculate average network delay as long as we know generation and service rates, and the threshold value, NT_{low} , for switching the in-service queue.

For use later in comparing the average delays for the case when all nodes are homogeneous, we derive the equivalent homogeneous node delay equation to

(7) for the link switching case by substituting c for c_i and λ for λ_{ij} :

$$\bar{T}_{switching} = \frac{1}{c} + \frac{\lambda}{c(c-\lambda)} + t_s \left(\frac{c-\lambda}{c-2\lambda} \right). \quad (28)$$

Using $\rho = \lambda/c$, this equation becomes

$$\bar{T}_{switching} = \frac{1}{c(1-\rho)} + t_s \left(\frac{1-\rho}{1-2\rho} \right). \quad (29)$$

2.2.3 Ten Node Packet Forwarding Operation

Our model approach for packet forwarding in the ten node ring will be to assume that each queue operates as an $M/M/1$ queue and use the delay equations for each link derived in (Taggart et al., 2005). We will sum the delays over all links, assuming that each link is weighted equally. Thus, total delay is given by

$$T_D(c_i) = \sum_{i=1}^{10} \frac{1}{c_i - AR_i}, \quad (30)$$

where c_i is the capacity and AR_i the arrival rates at each Node i . Arrival rate is given by

$$AR_i = G_i + \bar{P}_i - RX_i, \quad (31)$$

where G_i is the generation rate of packets, RX_i is the receive rate of packets, and \bar{P}_i is the offered load at Node i .

2.2.4 Ten Node Switching Operation

The approach for modeling the effect of switching behavior on delay in the ten node UWB ring is more complex. We still sum the delays in each node to arrive at total delay. Nodes 3 and 7 behave as servers with vacations, but when the ring is switched to send packets from Node 3 to Node 8, the offered loads to all nodes change as well. For example, Nodes 4 and 8, while served constantly go through periods when the offered load to each node goes to zero. This occurs when Nodes 3 and 7 stop sending traffic, for example when they are synchronizing with Nodes 4 and 8. Our approach is to calculate delays for each node in each network state defined in Fig. 7 and sum for each based on the duration spent in each state of operation. In this discussion acquisition time, t_{acq} , is the same as synchronzation time, t_{sync} , for the three node model.

For all nodes but 3 and 7, the delay formula in (30) works well, but because of the way the network operates with Node 3 having two queues, the bottom half nodes (4, 5, 6, 7) never forward any of the traffic bound for the top half nodes (1, 2, 8, 9, 10) from Node 3. Node 3 holds on to all of this traffic to send directly to. Node 8 after the link switching operation. The arrival rate in the queue, AR_i , for each of these nodes changes as the network changes state. For the four states shown in Figure 7, here are the applicable delay equations for Node 1. All Nodes but 3 and 7 follow similarly.

Node 3 sending to 4 state:

$$T_1^{3to4} = \frac{1}{c_1 + RX_1^{3to4} - \overline{P}_1^{3to4} - G_1} \quad (32)$$

Node 3 sending to 8 state:

$$T_1^{3to8} = \frac{1}{c_1 + RX_1^{3to8} - \overline{P}_1^{3to8} - G_1} \quad (33)$$

Acquisition state:

$$T_1^{acq} = \frac{1}{c_1 + RX_1^{acq} - \overline{P}_1^{acq} - G_1} \quad (34)$$

Wait state:

$$T_1^{wait} = \frac{1}{c_1 + RX_1^{wait} - \overline{P}_1^{wait} - G_1}. \quad (35)$$

To evaluate these equations, we define offered load matrix, T :

$$\mathbf{T} = \begin{bmatrix} 0 & \lambda_{1,2} & \lambda_{1,3} & \dots & \lambda_{1,10} \\ \lambda_{2,1} & 0 & \lambda_{2,3} & \dots & \lambda_{2,10} \\ \lambda_{3,1} & \lambda_{3,2} & 0 & \dots & \lambda_{3,10} \\ \vdots & \vdots & \vdots & \ddots & \vdots \\ \lambda_{10,1} & \lambda_{10,2} & \lambda_{10,3} & \dots & 0 \end{bmatrix} \quad (36)$$

where each $\lambda_{i,j}$ represents the average offered load in packets or bits per second between node i and node j in the network and 10 is the number of nodes in the network. We calculate the values for \overline{P}_i^{state} and RX_i^{state} by inspection from the offered load matrix, T . For example,

$$\begin{aligned} \bar{P}_1^{3to4} = & \sum_{i=4,5,6,7,8,9} \lambda_{i,1} + \sum_{i=4,5,6,7,8,9} \lambda_{i,2} + \sum_{i=4,5,6,7,8,9} \lambda_{i,3} + \sum_{i=4,5,6,7,8,9} \lambda_{i,4} \quad (37) \\ & + \sum_{i=6,7,8,9,10} \lambda_{i,5} + \sum_{i=7,8,9,10} \lambda_{i,6} + \sum_{i=8,9,10} \lambda_{i,7} + \sum_{i=9,10} \lambda_{i,8} + \lambda_{10,9} \end{aligned}$$

and

$$RX_1^{3to4} = \sum_{i=4,5,6,7,8,9,10} \lambda_{i,1}. \quad (38)$$

The task of calculating all these values is laborious, but not difficult. Nodes 3 and 7 behave differently, so we use another approach to calculate delays in each state. First, recall that Node 3 actually has two queues, so we must calculate delays for both queues. In addition, during the Acquisition and Wait states no packets are served in Nodes 3 and 7, so average delay for packets during this time is just 1/2 of the duration of the state. Finally, when Node 3 sends to Node 4, packets in the upper half queue in Node 3 do not get served, so the delay is 1/2 of the duration of the state. The converse is true when the upper half queue of Node 3 is operating and the lower half queue is without service. For convenience, we number the upper half queue in Node 3 as Queue 11. We write

$$T_3^{3to4} = \frac{1}{c_3 + RX_3^{3to4} - \bar{P}_3^{3to4} - G_3^{LH}} \quad (39)$$

$$T_3^{3to8} = \frac{1}{2} \left(\frac{N_3^H - N_3^L}{(c_3 - AR_3^U)} \right) \quad (40)$$

$$T_3^{acq} = \frac{1}{2} (2t_{acq}) \quad (41)$$

$$T_3^{wait} = \frac{1}{2} \left(t_{acq} + \sum_{i=1}^{10} \frac{1}{c_i} \right). \quad (42)$$

For Queue 11, the upper half queue in Node 3, we write

$$T_{11}^{3to4} = \frac{1}{2} \left(\frac{N_3^H - N_3^L}{(c_3 - AR_3^U)} + \sum_{i=1}^{10} \frac{1}{c_i} \right) \quad (43)$$

$$T_{11}^{3to8} = \frac{1}{c_3 + RX_3^{3to8} - \bar{P}_{11}^{3to8} - G_3^{UH}} \quad (44)$$

$$T_{11}^{acq} = \frac{1}{2} (2t_{acq}) \quad (45)$$

$$T_{11}^{wait} = \frac{1}{2} \left(t_{acq} + \sum_{i=1}^{10} \frac{1}{c_i} \right). \quad (46)$$

Finally, for Node 7 we write

$$T_7^{3to4} = \frac{1}{c_7 + RX_7^{3to8} - \overline{P}_7^{3to8} - G_7} \quad (47)$$

$$T_7^{3to8} = \frac{1}{2} \left(\frac{N_3^H - N_3^L}{(c_3 - AR_3^U)} \right) \quad (48)$$

$$T_7^{acq} = \frac{1}{2} (2t_{acq}) \quad (49)$$

$$T_7^{wait} = \frac{1}{2} \left(t_{acq} + \sum_{i=1}^{10} \frac{1}{c_i} \right). \quad (50)$$

For each state, we sum the delays in all nodes. Then we take the sum of the delays by state, weighting for the duration of each state.

$$\overline{T}_{overall} = W_{3to4} \sum_{j=1}^{11} \overline{T}_j^{3to4} + W_{3to8} \sum_{j=1}^{11} \overline{T}_j^{3to8} + W_{acq} \sum_{j=1}^{11} \overline{T}_j^{acq} + W_{wait} \sum_{j=1}^{11} \overline{T}_j^{wait} \quad (51)$$

where

$$W_{state\ i} = \frac{Duration_{state\ i}}{\sum_{all\ states\ i} Duration_{state\ i}} \quad (52)$$

2.3 Simulation Models

We use MATLAB to develop event-based simulation models for the three node network in both packet forwarding and in link switching operation. At this time, the simulation models for the ten node network are still in progress, we include only a preliminary comparison between the mathematical and simulation models for the ten node network.

2.3.1 Three Node Packet Forwarding Operation

Inputs to the model included average packet generation rates for packets, λ_{12} , λ_{13} , and λ_{23} and the average service rates at Nodes 1 and 2, c_1 and c_2 . Each simulation ran until 30,000 packets were received at nodes 2 and 3. We ran the simulation 50 times to obtain the average packet delay. We plotted error bars indicating the 95% confidence intervals of the data.

2.3.2 Three Node Switching Operation

The simulation model for three node switching operation was also written in MATLAB. Inputs to this model also included average packet generation rates for packets, λ_{12} , λ_{13} , and λ_{23} and the average service rates at Nodes 1

and 2, c_1 and c_2 . The model run duration depended on the number of queue switches desired. We ran the model for three to ten queue switching periods, but ignored the delay data from the first one to four switching periods to try to prevent system start up behaviors from affecting the delay data collected. We used the total number of received packets at nodes 1 and 2 as a secondary limit to the number of queue switches for the cases when short synchronization times allowed rapid switching between the queues. Again, when presenting the data, we plotted error bars indicating the 95 percent confidence intervals.

2.4 Selection of Modeled Parameters

2.4.1 Three Node Model

The plan and demonstrated data rates for UWB operation are about 500 Mb/s (Roy et al., 2004), which is nearly the same as the maximum 480 Mb/s rate specified for WiMedia UWB (ISO, 2007). Assuming an average packet length of 1500 bytes, this yields a transmission rate of 42,000 packets per second, therefore we choose our basic service rate to be 40,000 packets per second. To verify that models are applicable over a range of parameters, we also looked at situations with average service rates that were 50% higher, or 60,000 packets per second.

For continuous stable operation in the packet forwarding mode, the combined Node 1 packet generation rate, the sum of λ_{12} and λ_{13} , cannot exceed the average service rate at Node 1. This led to our choice of 15,000 packets per second as the basic average packet generation rate in each node.

Our choice of values for synchronization time were initially based on previous studies of UWB systems indicating that synchronization times were on the order of μs (ISO, 2007) to tens of ms (Roy et al., 2004). However, we quickly realized that for longer synchronization times (ms), packet forwarding would *always* achieve significantly less average packet delay than switching operation for our three node network. So, we needed to find an interesting operating point of this system where the combination of certain generation rates, service rates, and shorter synchronization times might make switching between nodes more desirable than simply forwarding packets through the established wireless links.

One very helpful way to identify this operating point is to use the mathematical models for packet forwarding and for link switching operation in the case of homogeneous nodes. By homogeneous, we mean that the nodes all have the same packet generation and service rates. By setting (7) for the forwarding

model equal to (29) and simplifying, we obtain:

$$t_{synch} = \frac{1 + 2\rho}{3c(1 - \rho)^2}. \quad (53)$$

When plotted in Fig. 8 for various service rates, c , and utilization factors ρ , this equation shows lines where the total average delay for forwarding packets is equal to the delay obtained when switching the links. For a given service rate and utilization, if the synchronization time used in the system is a bit smaller than the value on the equal delay line, a smaller delay will be incurred by switching links. If the synchronization time used in the system is a bit more than the equal delay line value, a smaller delay will occur when packets are forwarded without disturbing existing links.

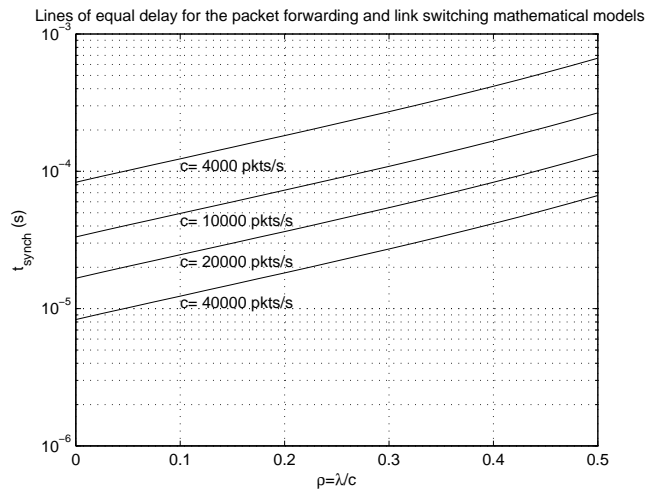


Fig. 8. Lines of equal delay for packet forwarding and link switching operation based on the mathematical models

In other words, this chart can be used to determine for our network whether for a given achievable synchronization time, the system should be set up to switch links or simply forward traffic without disturbing the links.

It is clear from Fig. 8 that for service rates characteristic of UWB networks, 40,000 packets per second, and for the utilization factor considered, $\rho \approx 0.375$, that acquisition times must be smaller than about $50 \mu s$ to tip the advantage towards switching links rather than simply forwarding the packets through the intermediate node. This observation helps us focus our modeling on interesting values of acquisition time.

Figure 9 shows us the same information in a more intuitive way by plotting average delay time as a function of the utilization factor, ρ , for different synchronization times. The average packet service rate is fixed at our standard 40,000 packets per second. The plot clearly shows that under these condi-

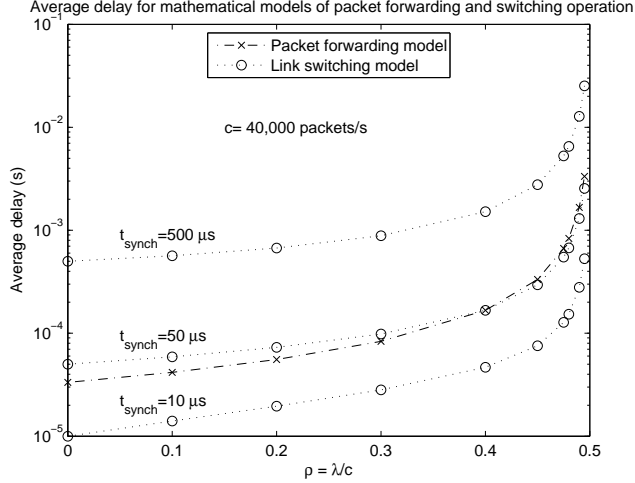


Fig. 9. Comparison of average packet delay for packet forwarding versus packet switching operation based on the mathematical models

tions, switching operation incurs less delay than forwarding operation only in the region

$$10\mu s \lesssim t_{synch} \lesssim 50\mu s. \quad (54)$$

The remaining problem, though, is that we don't know a priori how accurate the mathematical models are. If the models are accurate, this technique provides a useful way to determine the best mode of operation for the network. If the models are not accurate, utility decreases. We discuss the results of the models, including accuracy when compared to the simulation models in (3).

2.4.2 Ten Node Model

The ten node model assigns loads randomly in the offered load matrix, T , defined previously in Fig. 36. The offered loads, $\lambda_{i,j}$, are assigned randomly from a uniform distribution between 0 and 15,000 packets/s. The values for the high and low thresholds for the top half queue in Node 3 are variables. We keep the low threshold at zero and set the high threshold at between 5 and 20 packets. We set capacities for each node to values that provide aggregate capacity that exceeds the total offered load by a selectable amount. We look at cases for the aggregate capacity at 1.05, 1.01, and 1.005 times total offered load. Generally, we examined average delay for acquisition times from 0 to 5 μs , 0 to 50 μs , and 0 to 500 μs for the reasons given in the discussion of model parameters for the three node model.

3 Results

This section compares and explains the results of the mathematical and simulation results for the packet forwarding and the packet switching models.

3.1 Three Node Packet Forwarding Operation

The mathematical and analytical models for the three node network operating only by packet forwarding agreed very well, as shown in Table 4. The average delays agree very well and the 95% confidence interval is small in comparison with the mean delay.

Table 4

Average packet delay comparison for packet forwarding models

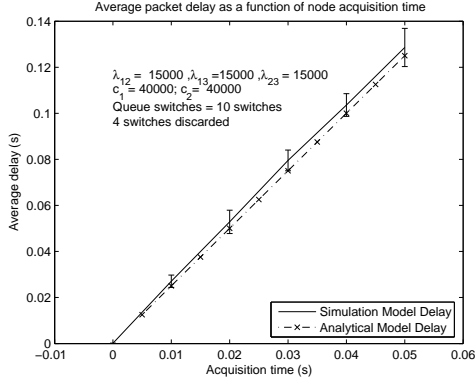
Model	Average Packet Delay	95% Confidence Interval
Mathematical	133.3 μs	NA
Simulation	133.6 μs	9.7 μs

3.2 Three Node Link Switching Operation

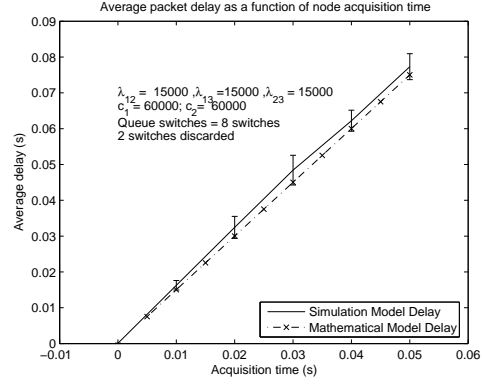
For longer synchronization times, the mathematical and simulation models for the three node network with link switching operation also agree well. Figure 10 shows good agreement between the mathematical model and the simulation model for synchronization times from 0 to 50 ms for two different average packet service rates.

The results for much shorter synchronization times do not match as well as for higher synchronization times. For synchronization times from 0 to 50 μs , Fig. 11 shows that the mathematical model underestimates the actual delay for the same values of average packet service rate.

The likely reasons for this mismatch becomes when we examine the average packet delays in each individual node. Fig. 12 compares the overall and individual queue delays for two cases. The left four plots are for a longer synchronization time - $t_{synch} = 50ms$. The right four plots are for a short synchronization time - $t_{synch} = 50\mu s$. Each group of four subplots shows the overall delay, the delay in Q_{12} , the delay in Q_{13} , and the delay in Q_{23} clockwise around the figure starting in the upper left quadrant.

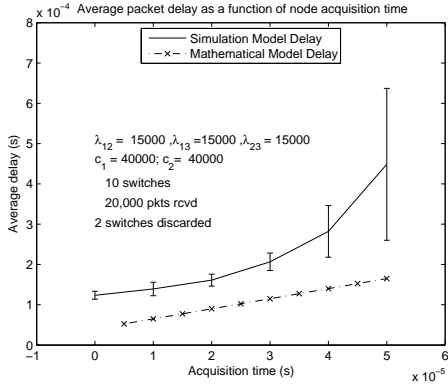


(a)

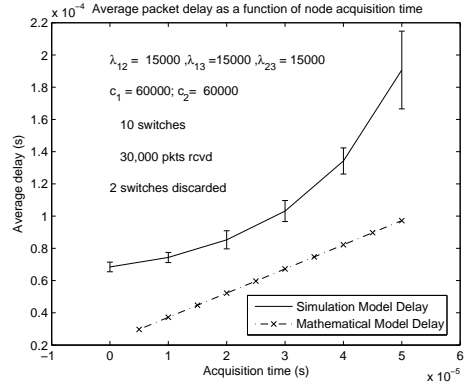


(b)

Fig. 10. Good agreement is seen in model comparisons for $t_{synch} = 50ms$ and two values of average packet service rate



(a)

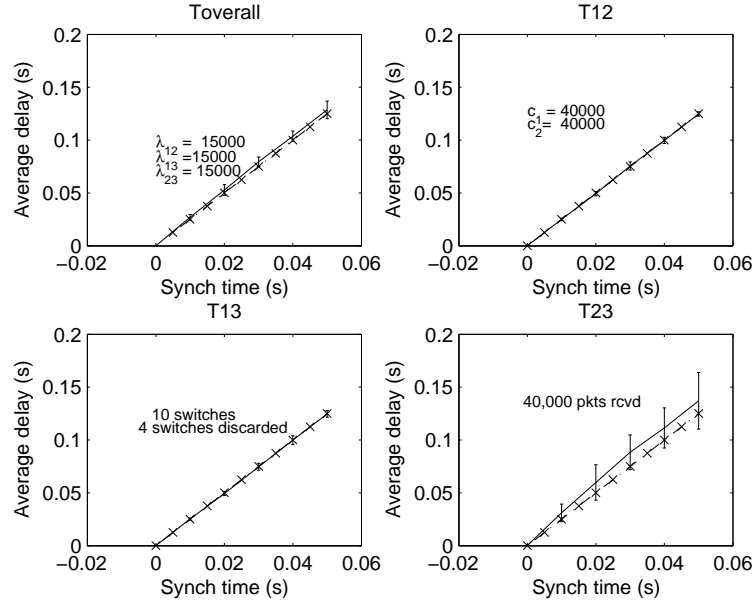


(b)

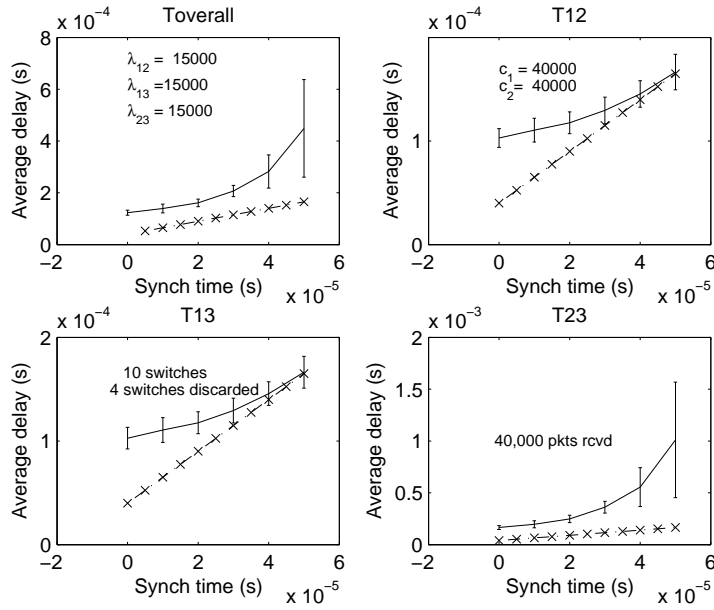
Fig. 11. The mathematical model underestimates delay in model comparisons for $t_{synch} = 50\mu s$ and two values of average packet service rate

In Fig. 12(a), for $t_{synch} = 50ms$, the mathematical and simulation models match well for Q12 and Q13, but not very well for Q23. In Fig. 12(b), the models don't match that well for Q12 and Q13, but the match is even worse in Q23.

The discrepancies arise from the assumptions used in the mathematical model regarding exhaustive service in the queues and achievement of steady state operation. In using the server with vacations model for queue operation, we inherit the implicit assumption that the queues are all exhaustively served. This is true for Q_{12} and Q_{13} in our model, but not exact for queue Q_{23} . Because Q_{23} only switches service when Q_{12} switches service, the service policy at Q_{23} is a limited service policy, not an exhaustive one. During a switching cycle, the number of packets in Q_{12} is always forced to zero at the end of the cycle by requiring exhaustive service of the queue. However, Q_{23} may still have packets in the queue, even when Q_{12} is empty. Even if generation and service rates



(a)



(b)

Fig. 12. Subplots of individual queue delays in model comparisons for $t_{synch} = 50ms$ and $t_{synch} = 50\mu s$.

are the same for the two queues, over many queue switches, Q_{23} may retain a backlog of packets, and therefore with a longer average delay for each packet.

Also implicit in the derivation of our mathematical delay model is the idea that each queue is effectively in steady state and that the maximum queue

size of each queue is approximately constant from cycle to cycle. This allowed us to set up and solve the simultaneous equations for delay in Section 2.2.2, but assumed that queues were in *equilibrium*. For very short synchronization times, the queues may not reach this equilibrium condition before service is switched. Thus, our mathematical delay formulation underestimates the actual delays seen in the simulation model results.

3.2.1 Ten Node Network

There are three factors that influence the delay performance of the ten node model: the high switching threshold for the top half queue in Node 3, H_3^H , the excess capacity ratio, B , and the acquisition time required for nodes to re-synchronize with a new link.

An interesting feature of the mathematical delay model for the ten node switching ring network is the non-linear shape of the delay plot, seen in Figure 13. This plot shows average delay for acquisition times between zero and 100 μs with excess capacity factor of 1.05 and a switching threshold of five packets. Intuitively, we expect delay to increase monotonically with acquisition time, but the plot shows a slight decrease in average delay for increasing acquisition time for a small region of acquisition times. The parabolic shape of the delay curve is due to the effect of weighting and summing the individual delays to obtain total average delay. As the acquisition time increases from zero, the delays in the *Node 3 sending to 4* and *Node 3 sending to 8* states of Figure 7 increase, but are weighted less because the duration of these states become increasingly short as compared to the *Acquisition* and *Wait* states. The weighting effect dominates at first causing the total delay curve to slope slightly downwards. Over time, however, the decrease in weighting due to increasing acquisition time is overcome by the fact that actual delays in all states are increasing or remaining constant as the acquisition time increases. This causes the total delay to ramp up again. As we will see, this effect does not seem to occur in the simulation model.

Fig. 14 shows the effect of excess capacity and queue switching threshold on the ten node network with acquisition times ranging from zero to five milliseconds. For longer acquisition times, neither excess capacity nor the value chosen for the switching threshold significantly affects the average delay. For these cases, the packet forwarding ring network outperforms the ring with switching nodes except for very short acquisition times. The effect of excess capacity and the switching threshold are greatly outweighed by the large acquisition time. In fact, comparing Fig. 14 with Fig. 10 for the simple three node switching model shows that even the effect of the number of nodes in the network on delay is overshadowed by large acquisition delays.

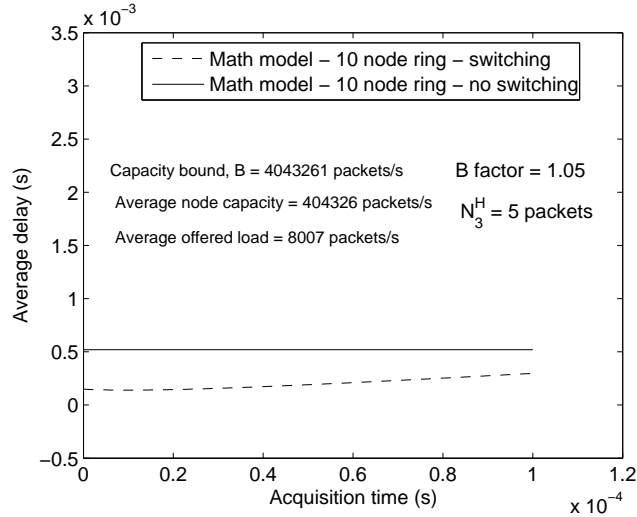


Fig. 13. Ten node network delay versus threshold value-short acquisition times

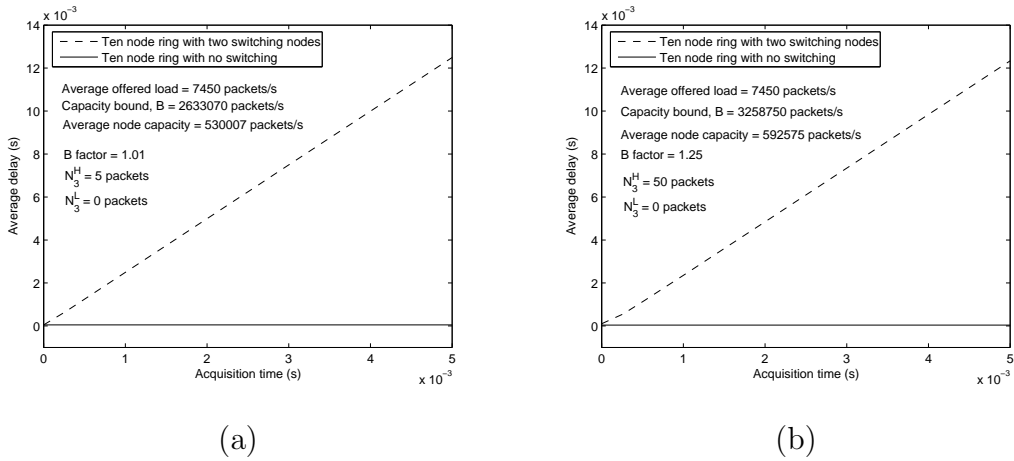
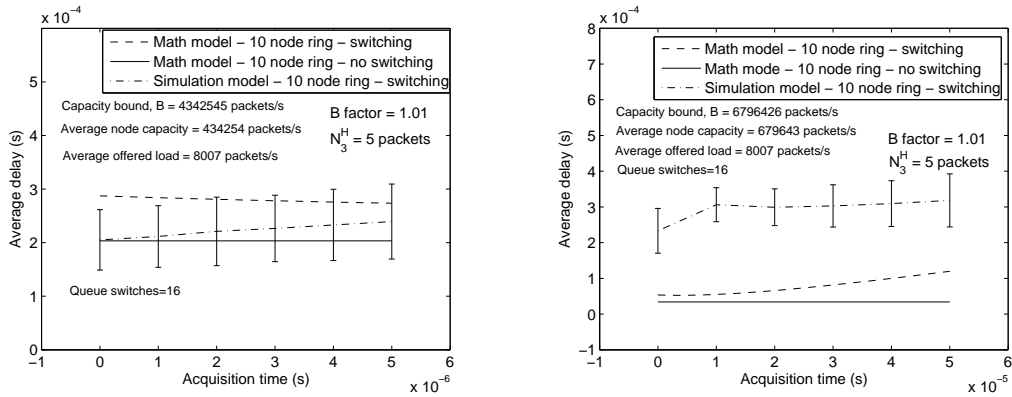


Fig. 14. Ten node network delay versus capacity excess at longer acquisition times

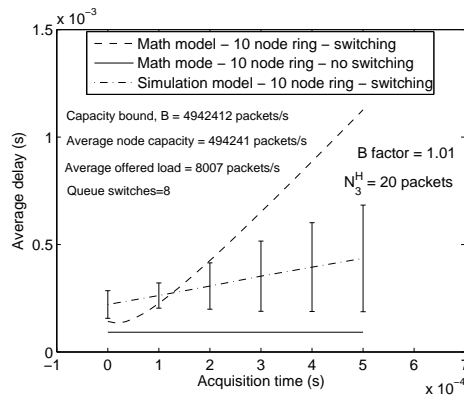
We developed an event-based simulation model in MATLAB for the ten node switching model. The three factors that influence the delay performance of the ten node switching network model are the high switching threshold for the top half queue in Node 3, N_3^H , the excess capacity ratio, B , and the acquisition time required for nodes to re-synchronize with a new link. We looked at these factors by analyzing model results in three acquisition time regimes: 0 to 5 μs , 0 to 50 μs , and 0 to 500 μs . We provide plots and a summary of selected results here.

Figure 15 shows the average delay as a function of acquisition time for the case when excess capacity is 1.01 times the total offered load. The capacity bound is the excess capacity factor times the total network capacity. The average node capacity is the capacity bound, B , divided by the total number of network nodes. The average offered load is the average $\lambda_{i,j}$ value from the traffic matrix, T . The top dotted line is the mathematical model prediction



(a)

(b)



(c)

Fig. 15. Model performance comparisons for average network delay as a function of node acquisition delay

of average delay as a function of acquisition time. The solid straight line is the mathematical model prediction of average packet delay for the packet forwarding ring with no switching. The hashed line in the middle with 95 percent confidence bars is the simulation model delay versus acquisition time.

In Figure 15(a), for acquisition times on the order of 0 to 5 μs , the average delay from the simulation model is comparable to the mathematically modeled delay for a switched network with these parameters. However, the delay predicted by the mathematical model for the packet forwarding ring network is quite a bit lower than the delay modeled for the switching network.

In Figure 15(b) acquisition times are on the order of 0 to 50 μs . The mathematical model for average delay for the switched ten node network is not far off from the delays predicted for the forwarding ten node ring. However, the simulation model for packet switching yields a higher average delay. Overall, the models predict that forwarding operation in the ten node ring will have the smallest average delay.

Finally, in Figure 15(c) acquisition times are on the order of 0 to 500 μs and the switching threshold is 20 packets versus 5. The mathematical and simulation model delay predictions for the switched ring network begin to diverge. The delay calculated by the mathematical model for the switching network shows a steeper increasing slope than that of delays obtained using the simulation model. The mathematical model for the forwarding ring network provides the smallest delay.

4 Conclusions

The paper derives mathematical and simulation models for the average packet delay for two types of operation for a simple UWB network of three nodes without a UWB MAC layer. The paper also describes a mathematical model for a ten node ring network in which one node can switch between delivering packets to its downstream neighbor and delivering packets to its the opposite node on the ring. For the three node models, forwarding packets through the intermediate node to the last node achieved the shortest average delay. However, when the synchronization time needed to support switching wireless links between nodes is very small, the network may incur less delay by switching links. We showed good agreement between mathematical and simulation-based models of average network delay at longer synchronization times. However, at very short synchronization times the mathematical model underestimates average packet delay, mainly because of the assumption of an exhaustive service policy in Q_{23} implicit in the server with vacations model. Contributing to this inaccuracy was the additional approximation of equilibrium queue operation that loses its accuracy for very short synchronization times.

For the ten node ring network, we showed the effect of switching threshold, excess capacity, and acquisition time on average packet delay. These effects show that for small acquisition times, the switching model can deliver packets with delay comparable to simply forwarding packets around the ring. We also showed that large synchronization times overshadow effects of the switching threshold and excess capacity and recognized that the mathematical model results were very similar for the three node and ten node models for large acquisition times. Finally, we included a comparison between the ten node mathematical delay model and delay results obtained from our simulation model for the network. This comparison showed comparable delays between the simulation model and the mathematical model for small acquisition times on the order of 5 μs . For longer acquisition times, 50-500 μs , the average delay predicted for the packet forwarding model is significantly less than delays from the simulation model of the packet switching topology.

References

- Aedudodla, S., Vijayakumaran, S., Wong, T., 2004. Rapid ultra-wideband signal acquisition. *Wireless Communications and Networking Conference, 2004 IEEE*), 1148–1153.
- Aedudodla, S., Vijayakumaran, S., Wong, T., 2006. Ultra-wideband signal acquisition with hybrid ds-th spreading. *IEEE Transactions on Wireless Communications*) 5 (9), 2504–2514.
- Bertsekas, D., Gallager, R., 1992. *Data Networks*. Prentice Hall, New Jersey.
- ISO, March 2007. International Standard ISO/IEC 26907 – Information technology – Telecommunications and information exchange between systems High Rate Ultra Wideband PHY and MAC Standard. International Standards Organization, Geneva.
- Roy, S., Foerster, J., Somayazulu, V., Leeper, D., 2004. Ultrawideband radio design: The promise of high-speed, short range wireless connectivity. *Proceedings of the IEEE*) 92 (2), 295–311.
- Scholl, M., Kleinrock, L., 1983. On the $m/g/1$ queue with rest periods and certain service-independent queuing disciplines. *Operations Research* 31 (4), 705–719.
- Taggart, C., Viniotis, Y., Sichitiu, M., 2005. Minimizing average network delay for ultra-wideband wireless networks. *Wireless Communications and Networking Conference, 2005 IEEE*) 4, 2276–2280.
- Taggart, C., Viniotis, Y., Sichitiu, M., 2007. The effect of node synchronization times in ultra wideband wireless networks. *Proceedings of the 10th ACM Symposium on Modeling, Analysis and Simulation of Wireless and Mobile Systems*, 306–313.